Journal of Hydraulic Research

ISSN: 0022-1686 (Print) 1814-2079 (Online) Journal homepage: http://www.tandfonline.com/loi/tjhr20

Dam-break flows over mobile beds: experiments and benchmark tests for numerical models

Sandra Soares-Frazão , Ricardo Canelas , Zhixian Cao , Luis Cea , Hanif M. Chaudhry , Andres Die Moran , Kamal El Kadi , Rui Ferreira , Ignacio Fraga Cadórniga , Noemi Gonzalez-Ramirez , Massimo Greco , Wei Huang , Jasim Imran , Jérôme Le Coz , Reza Marsooli , André Paquier , Gareth Pender , Marianeve Pontillo , Jeronimo Puertas , Benoit Spinewine , Catherine Swartenbroekx , Ryota Tsubaki , Catherine Villaret , Weiming Wu , Zhiyuan Yue & Yves Zech

To cite this article: Sandra Soares-Frazão , Ricardo Canelas , Zhixian Cao , Luis Cea , Hanif M. Chaudhry , Andres Die Moran , Kamal El Kadi , Rui Ferreira , Ignacio Fraga Cadórniga , Noemi Gonzalez-Ramirez , Massimo Greco , Wei Huang , Jasim Imran , Jérôme Le Coz , Reza Marsooli , André Paquier , Gareth Pender , Marianeve Pontillo , Jeronimo Puertas , Benoit Spinewine , Catherine Swartenbroekx , Ryota Tsubaki , Catherine Villaret , Weiming Wu , Zhiyuan Yue & Yves Zech (2012) Dam-break flows over mobile beds: experiments and benchmark tests for numerical models, Journal of Hydraulic Research, 50:4, 364-375, DOI: 10.1080/00221686.2012.689682

To link to this article: https://doi.org/10.1080/00221686.2012.689682

IAHR AIRH
Taylor & Francis
Taylor & Francis Group

Journal of Hydraulic Research Vol. 50, No. 4 (2012), pp. 364–375
http://dx.doi.org/10.1080/00221686.2012.689682

Research paper

Dam-break flows over mobile beds: experiments and benchmark tests for numerical models

IAHR Working Group for dam-break flows over mobile beds[†]

SANDRA SOARES-FRAZÃO, Associate Professor, *Civil and Environmental Engineering, Institute of Mechanics, Materials and Civil Engineering (IMMC), Université catholique de Louvain, Place du Levant 1, B-1348 Louvain-la-Neuve, Belgium.*
Email: sandra.soares-frazao@uclouvain.be (author for correspondence)

ABSTRACT
In this paper, the results of a benchmark test launched within the framework of the NSF–PIRE project "Modelling of Flood Hazards and Geomorphic Impacts of Levee Breach and Dam Failure" are presented. Experiments of two-dimensional dam-break flows over a sand bed were conducted at Université catholique de Louvain, Belgium. The water level evolution at eight gauging points was measured as well as the final bed topography. Intense scour occurred close to the failed dam, while significant deposition was observed further downstream. From these experiments, a benchmark was proposed to the scientific community, consisting of blind test simulations, that is, without any prior knowledge of the measurements. Twelve different teams of modellers from eight countries participated in the study. Here, the numerical models used in this test are briefly presented. The results are commented upon, in view of evaluating the modelling capabilities and identifying the challenges that may open pathways for further research.

Keywords: Benchmark test; dam break; experiment; numerical simulation; sediment

1 Introduction

Fast transient flows induced by the breaking of a dam or any control structure seriously affect the neighbouring population, causing loss of lives and important material damage. For an erodible bed, intense sediment transport occurs, reaching in cases an order of magnitude that is similar to the amount of transported water (Capart 2000). The associated morphological changes can be such that the entire valley is reshaped, as, for example, that which had occurred during the 1996 dam-break flood along the Ha!Ha! River in Quebec (Brooks and Lawrence 1999, Capart *et al*. 2007).

One of the consequences of the global climate change is an increased risk of failure for structures that were designed for discharges and precipitations often being no more adapted to the current conditions. Many research initiatives have recently been devoted to related questions (e.g. the European project FLOOD*site*). Numerical models are used to assess the consequences of a potential failure. However, most of the studies are conducted assuming pure hydrodynamic flows, that is, neglecting morphological effects (e.g. Hervouet and Petitjean 1999, Valiani *et al*. 2002, Nguyen *et al*. 2006, Roger *et al*. 2009). In this framework, the shallow-water equations appear as a well-established choice, and most of the existing models developed to solve these equations are able to produce valuable results for flood prediction.

Intense sediment transport increases the level of uncertainty of the simulation results. While it is generally agreed that an equation stating the conservation of the sediment mass should be added to the hydrodynamic equations, open questions exist regarding the inertia of moving sediment, the closure models for the transport rate or the necessary simplifications to represent the complex reality of actual sediment–fluid interactions in a mathematical model. To test and validate the modelling options for fast transient flows involving sediment transport, both laboratory and field data are needed. The latter data sets are scarce (yet see, e.g. Capart *et al*. 2007) and often affected by uncertainties. Possible sources of uncertainty are related to the initial conditions, the discharge, the estimation of the maximum water level or the roughness coefficients and sediment characteristics. Therefore, laboratory data are of paramount importance for validation purposes. At the laboratory scale, it is possible to focus on a limited set of parameters, to accurately control

[†] A detailed list of authors is provided at the end.
Revision received 26 April 2012/Open for discussion until 28 February 2013.

ISSN 0022-1686 print/ISSN 1814-2079 online
http://www.tandfonline.com

the test conditions and to repeat the experiment to enhance the data set.

This study aims to provide test cases to validate numerical models for the simulation of dam-break flows over a mobile bed. The test cases consist of dam-break flows issued from a 1-m breach flowing into a 3.6-m wide flume over a mobile bed made of uniform coarse sand. The tests were proposed to the scientific community as a blind benchmark, that is, as a modelling exercise without any prior knowledge of the measurements. Only the initial conditions were provided. Twelve modeller teams from eight countries participated in the study. Their results were compared with the experimental measurements during a workshop held in November 2010 in Louvain-la-Neuve, Belgium, within the frame of the NSF–PIRE project (Grant No. OISE 0730246) entitled "Modelling of Flood Hazards and Geomorphic Impacts of Levee Breach and Dam Failure" and under the auspices of the IAHR Fluvial Hydraulics Committee. Detailed information can be found at http://www.uclouvain.be/373040.html. The concerted analysis of the numerical results obtained without any model calibration is valuable in view of estimating the capabilities of current simulation tools for dam-break flows over mobile beds.

This paper presents the two test cases proposed as benchmark tests including the available experimental data. Then, significant aspects of the comparison between the numerical models and the experimental data are illustrated, based on the simulation results of the benchmark session. Finally, conclusions are drawn on the modelling options, the capabilities of current numerical models and the need for further research to improve such models.

2 Experiments

2.1 *Experimental set-up*

The experiments were conducted at the Hydraulics Unit of the LEMSC (Mechanical and Civil Engineering Laboratory, Université catholique de Louvain, Belgium). The flume was 3.6 m wide and about 36 m long, from which the useful length was about 27 m (Fig. 1). In Fig. 1, the breached dam is represented by two impervious blocks and a 1-m-wide gate located between the blocks. The origin of the axes is taken at the gate centre.

An 85-mm-thick sand layer was added onto the rigid flume bed. As shown in Fig. 1, it extended over 9 m downstream of the gate and over about 1.5 m upstream of it. The sand was not compacted and levelled by shifting a rigid beam. Downstream, the sand layer was held in place by a rigid sill whose height was equal to the initial sand thickness. The uniform coarse sand was characterized by $d_{50} = 1.61$ mm, relative specific gravity $\rho_s/\rho_w = 2.63$ and initial porosity $\varepsilon_0 = 0.42$, as evaluated from sampling after deposition. The Manning roughness coefficient

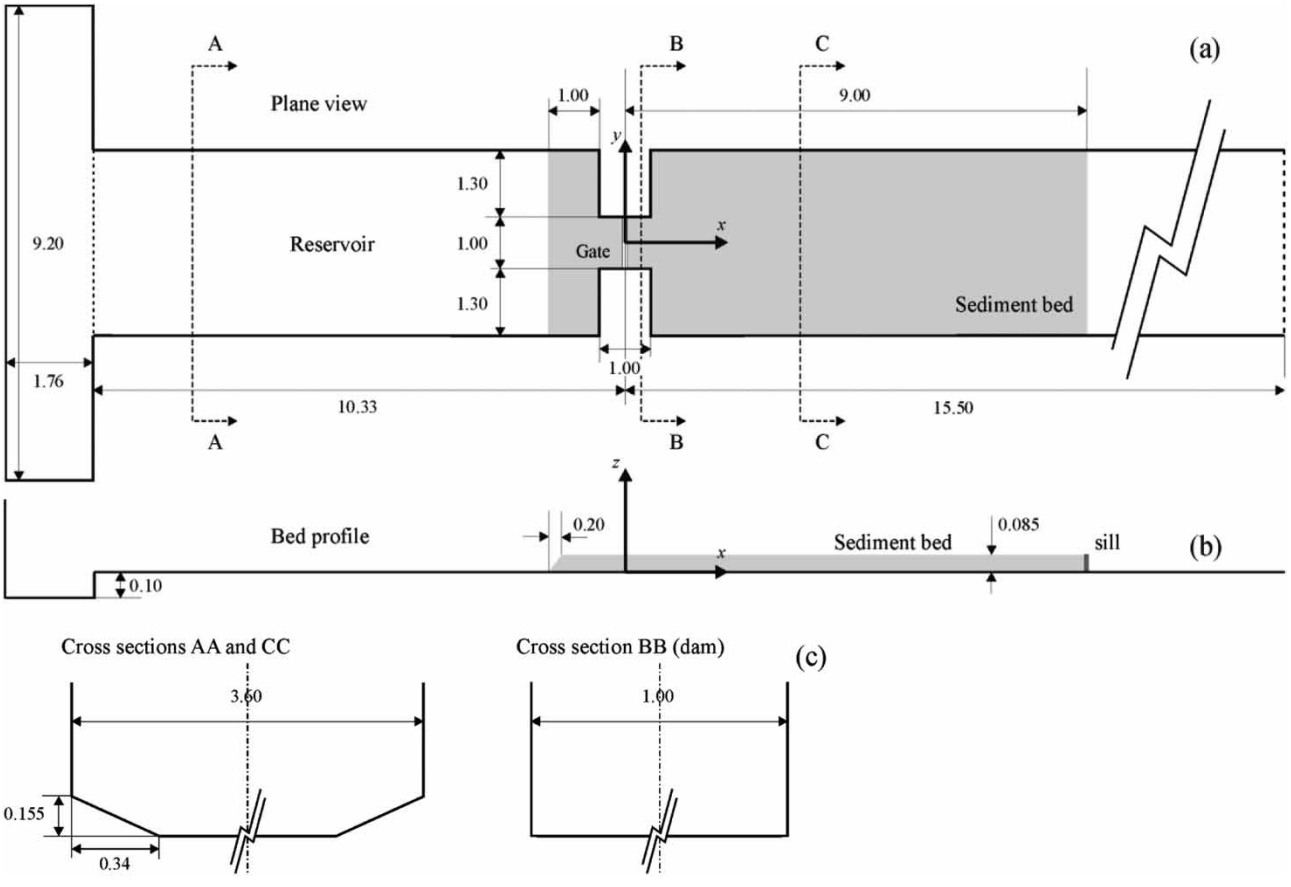

Figure 1 Flume dimensions (in metres): (a) plane view, (b) elevation and (c) cross-sections

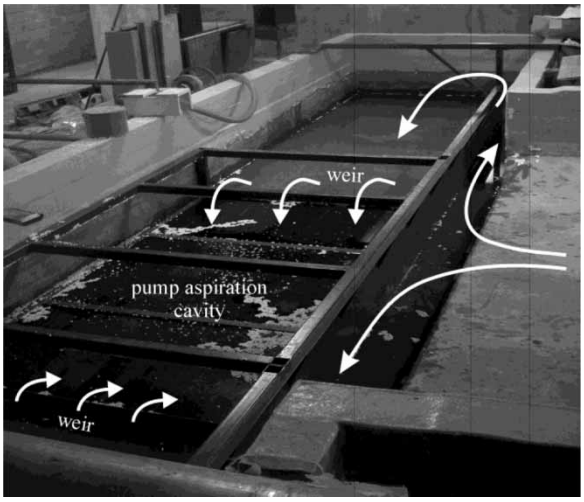

Figure 2 Downstream end of a flume

Table 1 Test conditions

	z_0 (m)	z_1 (m)	z_2 (m)	h_s (m)
Case 1	0.470	0.085	0.000	0.085
Case 2	0.510	0.150	0.150	0.085

for the sand was measured under uniform flow conditions as $n = 0.0165\,\mathrm{s/m^{1/3}}$, while it was observed from previous experiments that a value of $n = 0.010\,\mathrm{s/m^{1/3}}$ applies for the fixed bed.

The physical boundary conditions consisted of a closed wall at the upstream flume end and of a sediment trapping disposal at its downstream end, as shown in Fig. 2. It consisted of a primary weir diverting the flow towards the flume sides to slow down the water sufficiently for the sediment to deposit. The system was designed in a manner that all the sediment deposited in front of the primary weir. Should grains travel further, they can still deposit in the side areas. The effect of this downstream boundary condition (DBC) on the test results is discussed below.

2.2 *Test conditions*

The experiments consisted in filling up the upstream reservoir with water, adjusting if necessary the water level downstream of the gate and then triggering a dam-break wave by rapidly pulling up the gate. Two different cases were considered (Table 1). The initial water level in the upstream reservoir is denoted by z_0, while the initial water levels in the downstream portion (Fig. 1) are denoted by z_1 in the sand-covered area ($0\,\mathrm{m} < x < 9\,\mathrm{m}$) and by z_2 downstream of it ($x > 9\,\mathrm{m}$). Water levels were measured with reference to the fixed bed ($z = 0\,\mathrm{m}$). In both the cases, the initial sand layer of thickness $h_s = 0.085\,\mathrm{m}$ was initially saturated. For Case 1 with $z_1 = 0.085\,\mathrm{m}$ and $z_2 = 0\,\mathrm{m}$, the bed downstream of the sill was initially dry.

To simulate the dam break, the gate located 12 m from the upstream flume end was pulled up rapidly to reproduce an instantaneous scenario, using a mechanical counterweight system that

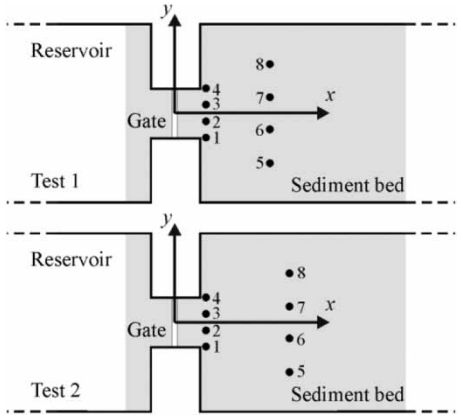

Figure 3 Gauge locations

Table 2 Gauge locations for Cases 1 and 2

	Case 1		Case 2	
Gauge no.	x (m)	y (m)	x (m)	y (m)
US1	0.640	–0.500	0.640	–0.500
US2	0.640	–0.165	0.640	–0.165
US3	0.640	0.165	0.640	0.165
US4	0.640	0.500	0.640	0.500
US5	1.940	–0.990	2.340	–0.990
US6	1.940	–0.330	2.340	–0.330
US7	1.940	0.330	2.340	0.330
US8	1.940	0.990	2.340	0.990

is much more rapid than a pneumatic jacket for this experimental scale. The opening time was measured as done in previous studies (Soares Frazão and Zech 2007) from digital high-frequency images. This opening time is defined as the time when the gate does not touch the water anymore, and it was found to be 0.23 s, corresponding to an instantaneous dam break (Vischer and Hager 1998) for both the initial conditions. The experiment was considered to last 20 s. Then, the gate was closed and the flow stopped. It was observed that the morphological evolution was comparatively small after that instant.

3 Available measurements

3.1 *Water level*

During the experiments, the temporal water level evolution was measured by means of eight Baumer™ ultrasonic probes of 12.5-Hz acquisition rate. The gauge locations are indicated in Fig. 3 and their exact positions are stated in Table 2.

Test repeatability was checked by comparing the measured water levels from different but identical experiments. From Fig. 4 (Case 1), it can be noted that a satisfactory level of repeatability resulted, given the intense sediment transport and morphological evolution. For each gauging point, the data acquired during 20 s at an irregular rate of about 9–16 Hz were first re-sampled each 0.1 s to eliminate the small lag due to the

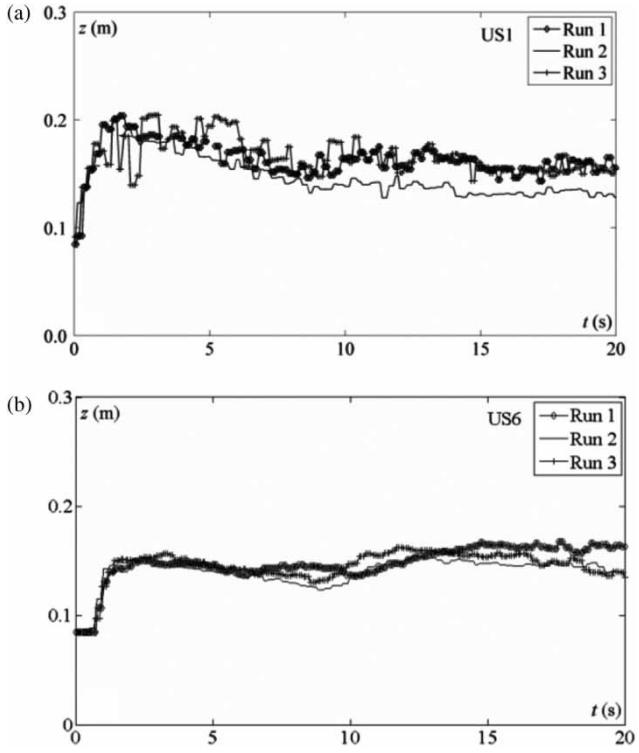

Figure 4 Repeatability of the water level measurements for three different runs of Case 1 at gauges (a) US1 and (b) US6

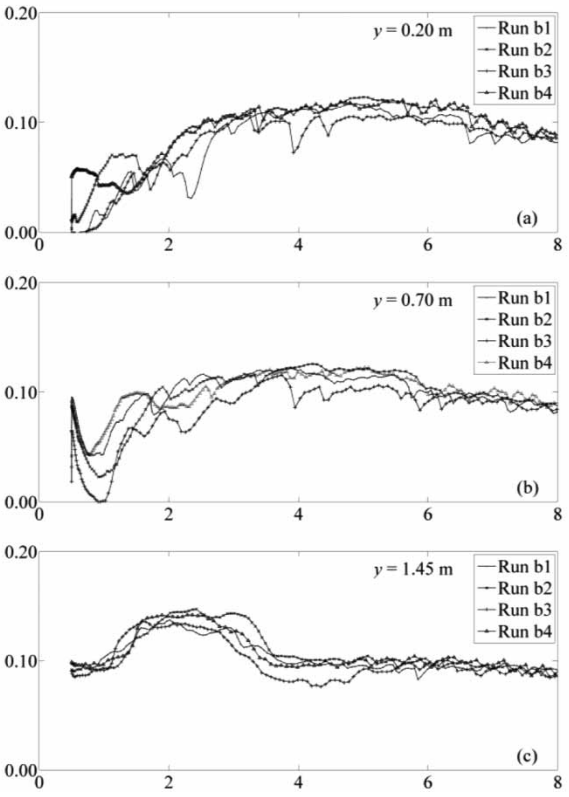

Figure 5 Repeatability of the bed elevation measurements for Case 1 from four different runs and three longitudinal profiles for y = (a) 0.20 m, (b) 0.70 m and (c) 1.45 m

measurement devices. Then, for each gauge, and for each time instant, the mean experimental value and the standard deviation were calculated. The mean standard deviation for each gauge was then calculated by averaging the values of the individual time steps to obtain the range of errors of the experimental data for the corresponding gauge. Following this procedure, for the ensemble of experiments, the mean observed standard deviation was between 0.006 and 0.016 m, depending on the considered gauge, with maximum values being between 0.018 and 0.032 m.

3.2 *Bed elevation*

During an experiment, it is impossible to follow the scour and deposition processes. After the passage of the dam-break wave that induced strong morphological changes, the experiment was stopped by closing the gate after 20 s. The bed elevation was then measured using a Delft bed profiler from $x = 0.5$ m to $x = 8$ m over the whole flume width with a spacing of $\Delta y = 0.05$ m.

As for the water level measurements, test repeatability was checked by comparing the measured bed profiles issued from different experimental runs. The result is illustrated for Case 1 in Fig. 5 for four runs. Note that a satisfactory level of repeatability was achieved. Using a procedure that was the same as that used for the water levels, the mean and maximum values of the standard deviation for the bed elevation measurements were found to be 0.008 and 0.029 m, respectively.

Combining the measured bed profiles, an elevation map for the final bed topography was reconstructed. For Case 1, this map in a perspective view is shown in Fig. 6(a). The intense scour ($z < 0.085$ m) immediately downstream of the failed dam is

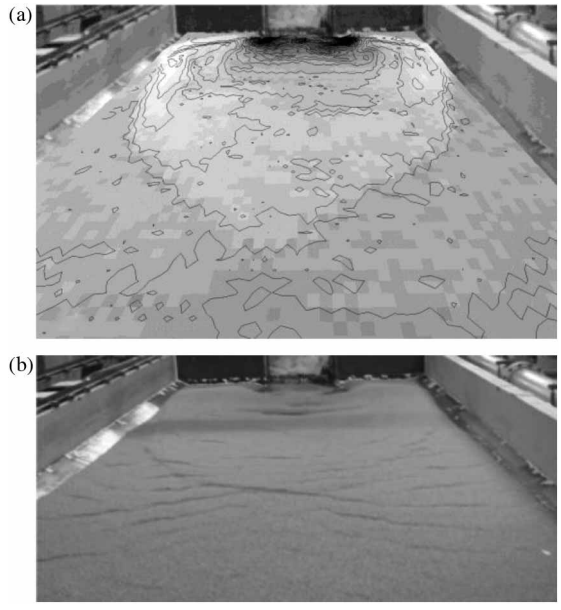

Figure 6 Final bed topography for Case 1: (a) perspective view from downstream, reconstructed from the measured bed profiles, and (b) photograph taken after water drainage at the end of the test

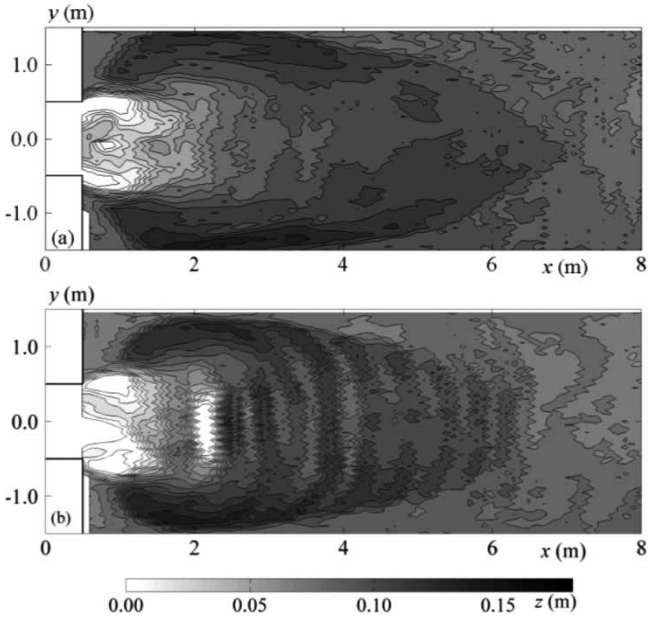

Figure 7 Final bed topography for (a) Case 1 and (b) Case 2, reconstructed from the measured bed profiles (contour lines spaced by 0.01 m)

clearly identified as well as the deposition area with a typical tongue shape. This is consistent with the photograph of the bed (Fig. 6b) taken at the end of the experiment, after slowly draining the water.

The final measured bed topographies for Cases 1 and 2 are shown in Fig. 7. The key difference between these is that in the latter, the bed topography shows the residual presence of antidunes that formed during the dam-break wave. After stopping the experiment, the amplitude of the bed forms decreased, yet a good trace of these remained (Fig. 7b).

4 Description of simulations

Twelve researchers or research teams (Table 3) provided simulation results for the two test cases. The simulations were conducted in a blind way, that is, without any prior knowledge of the experimental results. The information available to the modellers consisted of

- The dimensions of the flume (Fig. 1) and a photograph of the initial sediment bed.
- The initial conditions for Cases 1 and 2.
- The characteristics of the bed material: $d_{50} = 1.61$ mm, specific gravity $\rho_s/\rho_w = 2.63$ and porosity $\varepsilon_0 = 0.42$.
- The estimation of the Manning friction coefficients $n = 0.0165\,\mathrm{m}^{-1/3}$ s for the sand bed and $n = 0.010\,\mathrm{m}^{-1/3}$ s for the fixed bed.
- The free selection for DBC, to be simulated either as a free outflow or a closed wall. This degree of freedom was given because it was assumed that the DBC would not affect the morphological bed evolution during the limited test duration.

Table 3 Sources of detailed information of each model used for simulations

Modellers	Name	Reference
IST, Portugal	IST	Ferreira *et al*. (2009) and Canelas (2010)
Wuhan Univ., China	WUH	Cao *et al*. (2004)
Univ. La Coruña, Spain	COR	Cea and Vásquez-Cendón (2010) and Cea *et al*. (2009)
EDF-R&D, France	EDF	TELEMAC, Villaret *et al*. (2009)
FLO-2D, USA	RF2D	FLO-2D, Gonzalez-Ramirez (2010)
Univ. of Naples, Italy	UNA	Pontillo and Greco (2010)
IRSTEA, France	CEM	RUBAR 2.0, Bessenasse *et al*. (2004) and Paquier (2009)
Hiroshima Univ., Japan	HIR	Tsubaki and Fujita (2010) and Shige-eda *et al*. (2003)
UCL, Belgium (1)	UCL1	Soares-Frazão and Zech (2011)
UCL, Belgium (2)	UCL2	Spinewine (2005a, 2005b)
UCL, Belgium (3)	UCL3	Swartenbroekx *et al*. (2010)
Univ. of Mississippi, USA	MISS	Wu *et al*. (2009)

- Gauge locations for the two considered cases.

The details of the models used by each modeller or team can be found in the references listed in Table 3. A summary of the simulation models corresponding to the received results for the benchmark tests is provided in Table 4, based on the descriptions provided by the modellers within the framework of the benchmark.

Regarding the flow equations, most of the modellers use the shallow-water framework complemented with a transport equation for the sediment and the associated morphological evolution. This implies the mass conservation equation

$$\frac{\partial z_w}{\partial t} + \frac{\partial q_x}{\partial x} + \frac{\partial q_y}{\partial y} = 0 \tag{1a}$$

where z_w is the water level, h the water depth and $q_x = uh$ and $q_y = vh$ are the unit-width total discharges (i.e. water and sediment) in the x- and y-directions, respectively, with u and v being the depth-averaged velocity components. Considering the water phase only, this equation is sometimes simplified to

$$\frac{\partial h}{\partial t} + \frac{\partial q_{w,x}}{\partial x} + \frac{\partial q_{w,y}}{\partial y} = 0 \tag{1b}$$

Table 4 Summary of simulation models

Modellers	Name	Equations	Sediment closure	Num. sch.	Mesh	DBC
IST, Portugal Canelas and Ferreira (2010)	IST	Inert. coupl SW+Eq. (5)+NE	Ferreira *et al*. (2009) sheet flow formulae	FV Flux vector splitting	Triangles 0.01 m	W
Wuhan Univ., China Cao *et al*. (2010)	WUH	Mixture cont. and momentum	q_s: MPM	FV Approx. Riem. solver	Square 0.02 m	O
Univ. La Coruña, Spain Cea *et al*. (2010)	COR1	SW+Eq. (4)+NE	τ_c^*: Parker q_s: MPM	FV Roe	Rectangles 0.06 m	C
	COR2		τ_c^*: Parker q_s: Van Rijn			
	COR3		τ_c^*: Shields q_s: Van Rijn			
EDF, France Die Moran *et al*. (2010)	EDF1	SW+Eq. (4)	MPM	FE implicit for flow FV for sediment transport	Triangles 0.20 m Triangles 0.10 m	O
	EDF2					
FLO-2D, USA Gonzalez-Ramirez (2010)	RF2D1	SW+Eq. (4)	q_s: Ackers-White	FE Galerkin weighted residual method	Triangles 0.06 m	O
	RF2D2		q_s: MPM			
	RF2D3		q_s: Yang			
IRSTEA, France (former Cemagref) Paquier and Le Coz (2010)	CEM1	SW+Eq. (5)	τ_c^* 0.047, lag 1 m q_s: MPM	FV Roe second-order MUSCL	Rectangles 0.10 m	W/O
	CEM2		τ_c^* 0.047, lag 0.1 m q_s: MPM			W
	CEM3		τ_c^* 0.15, lag 1 m q_s: MPM			W
Univ. of Naples, Italy Pontillo and Greco (2010)	UNA1 UNA2	SW two-phase NE	Drag $C_d = 0.30$ Drag $C_d = 0.05$	FV Predictor -corrector	Rectangles 0.10 m	O
UCL, Belgium Soares-Frazão (2010)	UCL1	SW+Eq. (4)	q_s: MPM	FV HLL	Triangles 0.05 m	W
UCL, Belgium Spinewine (2010)	UCL2	Two-layer	Bed shear stress	FV HLL	Rectangles 0.02 m	W
UCL, Belgium Swartenbroekx (2010)	UCL3	Two-layer	Bed shear stress	FV HLL	Triangles 0.05 m	W
Hiroshima Univ., Japan Tsubaki (2010)	HIR	SW+Eq. (4)	q_s: Ashida-Michiue	FV FDS	Triangles 0.05 m	O
Univ. of Mississippi, USA Wu and Marsooli (2010)	MISS	GSW+Eq. (5)+NE	q_s: Wu, total load	FV HLL	Rectangles 0.025 m	O

where $q_{w,x}$ and $q_{w,y}$ are the unit-width water discharges. The momentum conservation equations read

$$\frac{\partial q_x}{\partial t} + \frac{\partial}{\partial x}\left(\frac{q_x^2}{h} + g\frac{h^2}{2}\right) + \frac{\partial}{\partial y}\left(\frac{q_x q_y}{h}\right) = gh(S_{o,x} - S_{f,x}) \quad (2)$$

$$\frac{\partial q_y}{\partial t} + \frac{\partial}{\partial x}\left(\frac{q_x q_y}{h}\right) + \frac{\partial}{\partial y}\left(\frac{q_y^2}{h} + g\frac{h^2}{2}\right) = gh(S_{o,y} - S_{f,y}) \quad (3)$$

where g is gravity acceleration, S_o the bed slope and S_f the friction slope. Again, the total unit discharges q_x and q_y are sometimes replaced by the water discharges only, that is, $q_{w,x}$ and $q_{w,y}$. For the sediment, two types of continuity equations are used: either the classical Exner equation (4) or an advection equation for sediment concentration such as the first of Eq. (5):

$$(1-\varepsilon_0)\frac{\partial z_b}{\partial t} + \frac{\partial q_{s,x}}{\partial x} + \frac{\partial q_{s,y}}{\partial y} = 0 \quad (4)$$

$$\frac{\partial hC}{\partial t} + \frac{\partial q_x C}{\partial x} + \frac{\partial q_y C}{\partial y} = E - D = -(1-\varepsilon_0)\frac{\partial z_b}{\partial t} \quad (5)$$

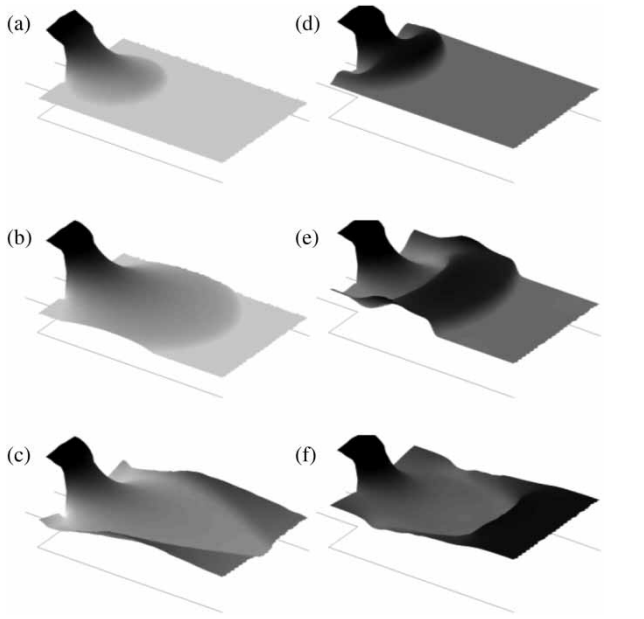

Figure 8 Computed water levels from UCL1 at $t = 1, 2$ and 5 s for Case 1 (a–c) and Case 2 (d–f)

In Eq. (4), z_b is the bed elevation, ε_0 the bed porosity and $q_{s,x}$ and $q_{s,y}$ are the unit-width sediment transport rates in the x- and y-directions, respectively. In Eq. (5), C is the depth-averaged sediment concentration, while E and D stand for the net erosion or deposition rates of a granular material. Alternatively, introducing either Eq. (4) or (5) into Eqs. (1a,1b)–(3) leads to fully-coupled equations (e.g. WUH reported by Cao *et al*. 2004). An alternative used at IST (Ferreira *et al*. 2009) consists in combining Eq. (5) with total mass conservation instead of with Eq. (1a,1b).

Where applicable, reference to Eqs. (1a,1b)–(5) is made in Table 4. Note that models based on the same set of equations may differ by the closure equations used to describe the sediment transport rate q_s (e.g. Meyer-Peter and Müller, Ashida-Michiue and Van Rijn) or the erosion and deposition rates E and D. Some models consider only bed load transport, while others consider a sediment concentration over the whole flow depth. Models such as MISS (Wu *et al*. 2009) consider the effects of sediment concentration and bed change in Eqs. (1a,1b)–(4), yielding the generalized shallow-water (GSW) equations coupled with a non-equilibrium sediment transport model.

Alternatively, two-layer models were used by some modellers (UCL2 used by Spinewine 2005b and UCL3 used by Swartenbroekx *et al*. 2010) to distinguish the movement of a clear water layer located above a layer consisting of a sediment–water mixture. These models use two mass conservation equations (water and sediment) and four momentum conservation equations (water and sediment in the x- and y-directions, respectively). A two-phase model (UNA used by Pontillo and Greco 2010) was also used where the solid and liquid phases were described by distinct movement equations. The latter two-layer and two-phase models explicitly consider the inertia of the mobilized

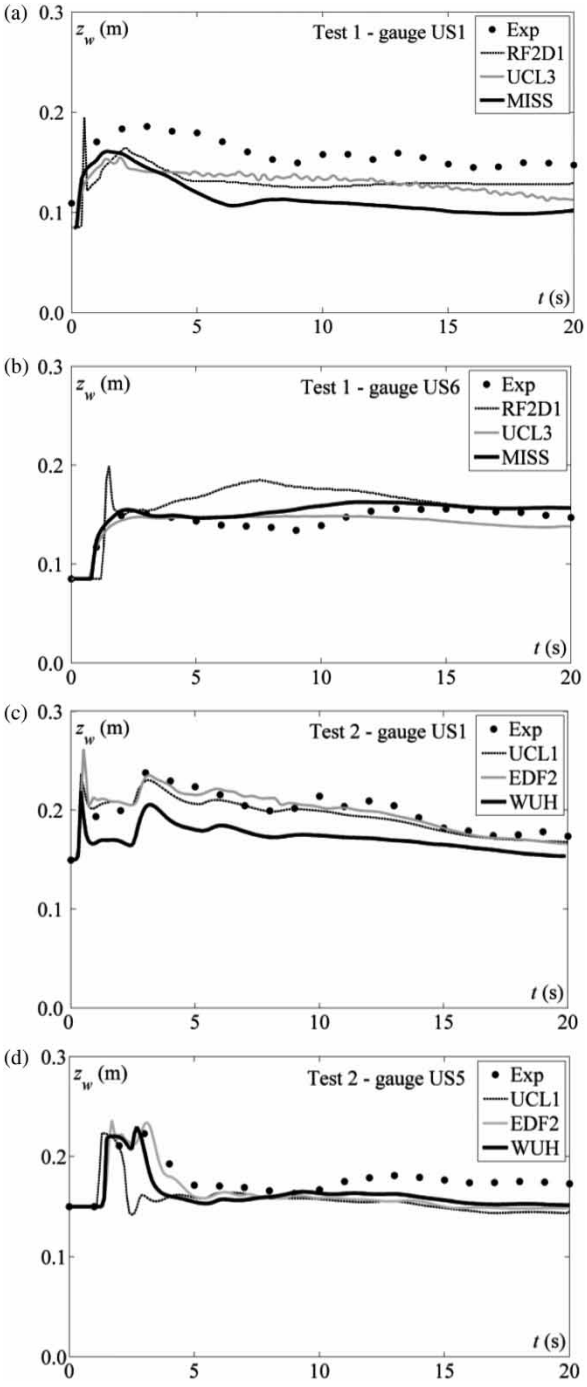

Figure 9 Measured and some computed water levels for Cases (a) 1-US1, (b) 1-US6, (c) 2-US1 and (d) 2-US5

sediments on the flow and have the particularity that no explicit closure equation is required for the sediment transport. Closure parameters concern either the drag coefficient (two-phase model UNA) or the interface shear stresses (two-layer models UCL2 and UCL3).

In Table 4, the acronym SW in the column "Equations" denotes the classical shallow-water equations (Eqs. 1a,1b–3), while the sediment transport equation is given by the equation number (Eq. 4 or 5) with an indication NE for non-equilibrium transport where appropriate; in the column "Sediment closure",

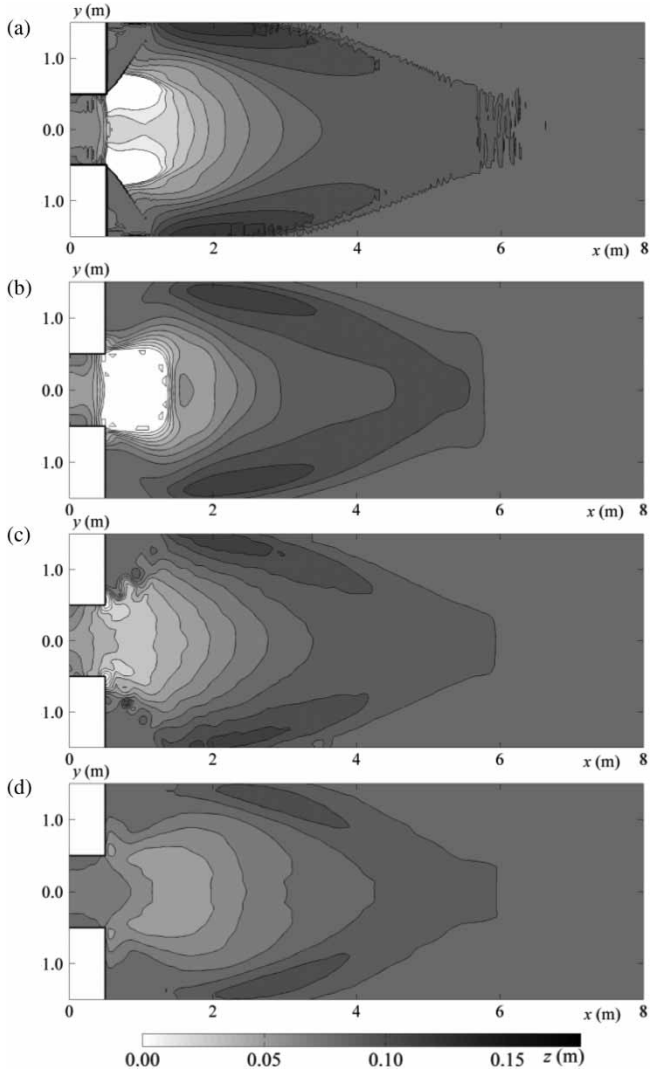

Figure 10 Computed bed topographies for Case 1: fine-mesh results provided by (a) WUH and (b) MISS and coarse-mesh results provided by (c) EDF2 and (d) UNA2

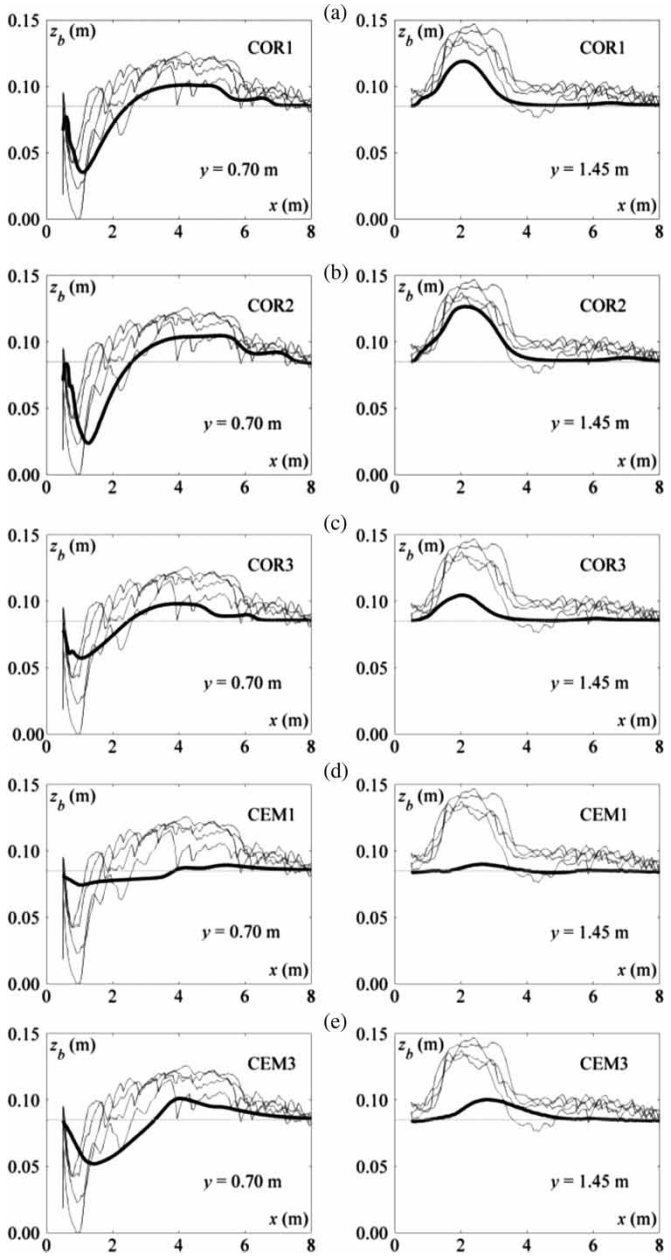

Figure 11 Effect of sediment transport formula and closure parameters analysed from the results reported by Cea *et al*. (a–c) and Paquier and Le Coz (d,e): (a) τ_c^* reported by Parker and q_s by Meyer-Peter and Müller, (b) τ_c^* reported by Parker and q_s by Van Rijn, (c) τ_c^* reported by Shields and q_s by Van Rijn, (d) $\tau_c^* = 0.047$ reported by Shields and q_s by Meyer-Peter and Müller and (e) $\tau_c^* = 0.15$ and q_s reported by Meyer-Peter and Müller. (—) experimental results and (—) numerical results

MPM denotes the Meyer-Peter and Müller formula for the sediment transport rate q_s, while "Parker" refers to the critical shear stress formula given by Parker *et al*. (2003); in the column "Numerical scheme", FV stands for finite volumes, FE for finite elements and HLL for the Harten–Lax–Van Leer flux calculation scheme; in the column "DBC", W refers to wall and O to open condition.

As for numerical models, most of the participants used finite-volume schemes. Only EDF and RF2D used FEs. The meshes are either unstructured triangular or square and rectangular structured grids. Different levels of refinement were considered, with the typical mesh dimension (edge length) ranging from 0.20 to 0.01 m in the area of interest immediately downstream of the dam.

For the DBC, as prescribed, either an open condition (O) or a closed wall (W) was used. It must be recalled that the experiment was stopped after 20 s by closing the gate since no more significant bed evolution occurred. For Case 1, this end time was such that the DBC did not affect the bed morphological evolution in the area of interest, as the back wave issued from the water reflection against the downstream wall did not have enough time to reach the concerned area. This was checked numerically by several modellers. For Case 2, the effect of the DBC arose earlier: for a closed wall condition, the back wave reaches the area of interest before the end of the experiment. As checked by several modellers, the consequences are significant for the water level but rather limited for the bed elevation.

5 Overview of the results

5.1 *General observations*

Despite the difficulty of the exercise, all the models provided valuable results, giving an idea of the ability of the current models to simulate a fast transient flow with significant morphological evolution. In some cases, the water level was predicted well, while the bed evolution was underestimated; in other cases, the bed evolution was better predicted than the water level.

As outlined in Table 4, different mesh refinements were used, with the consequence that different time steps were used. Some modellers used fixed time steps (e.g. EDF $\Delta t = 0.01$ s and MISS $\Delta t = 0.005$ s); others used variable time steps limited by a Courant-Friedrichs-Lewy (CFL) constraint (e.g. HIR CFL $= 0.1$, UCL1 CFL $= 0.9$, UCL3 CFL $= 0.5$ and CEM CFL $= 0.5$). Rather than ranking the numerical results according to the degree of likelihood with the experimental data, the most significant results were analysed to highlight the key issues to be further investigated for dam-break flows over mobile beds.

5.2 *Water level predictions*

Case 1 can be considered to be similar to a dam-break flow over an initially dry bed, while Case 2 would correspond to a flow over a wet bed. The first flow instants are illustrated for both test cases in Fig. 8 using numerical results obtained from the UCL1 model. The simulation qualitatively indicates the observed flow features: the two-dimensional (2D) wave expansion immediately downstream of the gate and the reflections against the lateral flume walls.

Figure 9 compares the selected numerical results and the measured water levels. For clarity of the figure, the experimental data were re-sampled each second. It can be observed that the results are generally better for Case 2 than for Case 1. This is particularly significant for the water level at gauge US1 (Fig. 9a,c), located close to the corner of the dam abutment, that is, in the area where 2D spreading effects of the wave are important. For Case 2, the formation of a bore upon arrival of the fast dam-beak wave in the downstream layer of water at rest was identified in the measurements and reasonably well reproduced by the numerical models (Fig. 9d).

5.3 *Bed level predictions*

The final bed topography was the key element of comparison in the benchmark tests. While all the models were able to predict the occurrence of scour immediately downstream of the gate and the shape of the deposition area, their amplitudes were usually underestimated (e.g. Case 1 in Fig. 10 compared with Fig. 7a). This underestimation appears to be more significant for the coarse-mesh results (Fig. 10c,d) than for the fine-mesh results (Fig. 10a,b).

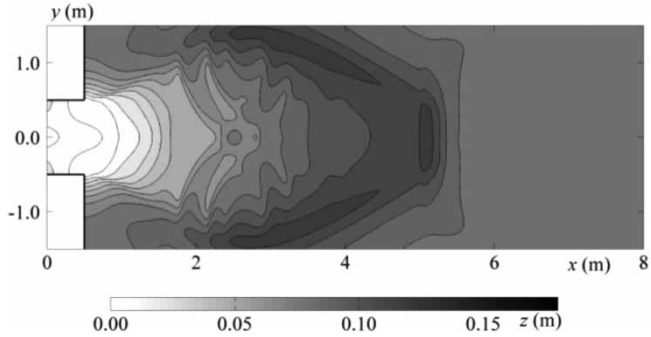

Figure 12 Bed topography at $t = 15$ s for Case 2 from UCL2 with indication of bed forms

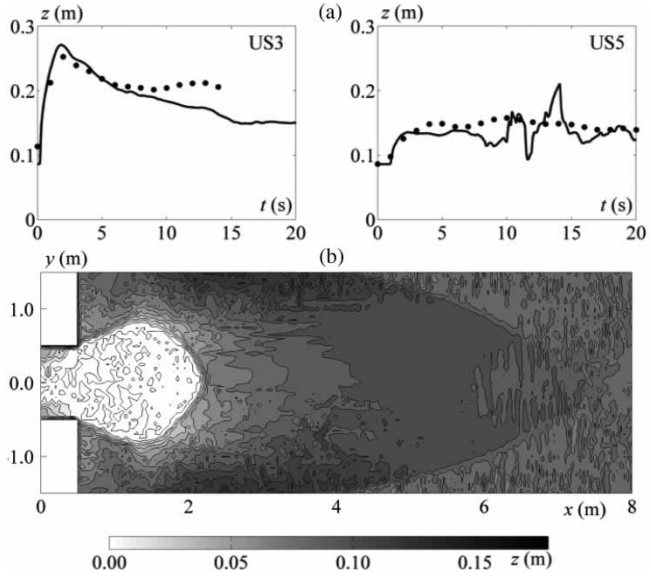

Figure 13 Computed results for Case 1 (HIR): (a) water level at gauges US3 and US5 with (•) experimental results and (—) numerical results and (b) final topography

5.4 *Effect of sediment transport formula*

Some modellers investigated the effect of the sediment transport formula and of parameters in the closure equations. Results are shown in Fig. 11 for Case 1 where the experimental profiles issued from the four experimental series shown in Fig. 5 are plotted as light lines to provide a visual indication of the range of variabilities. The computed results are plotted as a thick black line. Logically, the critical shear stress τ_c^* (threshold of sediment mobilization) appears to be a key parameter for bed material transport. Particularly, the critical shear stress formula given by Parker *et al*. (2003) leads to more intense transport than the classical value derived by Shields.

5.5 *Bed forms*

Due to the initial downstream water layer over the sediment bed, the wave propagation in Case 2 was such that antidune-type bed forms appeared (Fig. 7). Note that some models run on fine meshes qualitatively reproduce the formation of these bed forms, as shown for UCL2 at time $t = 15$ s in Fig. 12.

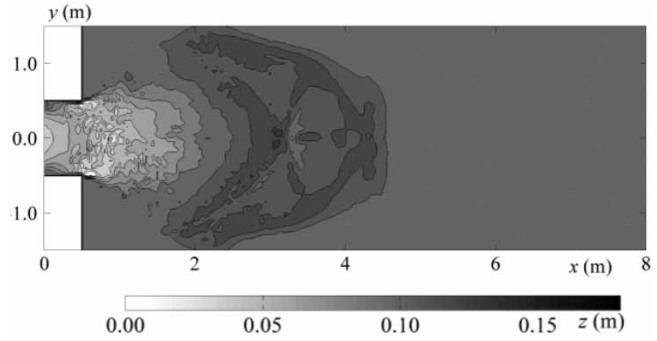

Figure 14 Final bed topography for Case 2 of IST

5.6 *Observed numerical difficulties*

Numerical instabilities were observed for some sets of results for various reasons, for example, the choice of the value for the drag parameter (UNA model), the level of coupling between the hydrodynamic and morphological equations and the limitation scheme for higher order methods. Note that the computed water level is usually much more affected than the computed bed elevation. In particular, the results HIR for Case 1 shown in Fig. 13 show a surprisingly good agreement with the final measured bed topography in terms of scour and deposition amplitudes, while the water level presents important oscillations, indicating yet unresolved instabilities.

However, irregularities that do not preclude a stable solution were observed in the results of IST for Case 2 (Fig. 14), where an indication of possible bed forms is also observed.

6 Conclusions

In this paper, a detailed experimental data set regarding two cases of 2D dam-break flows over mobile beds has been presented, together with the results of a benchmarking exercise consisting of blind simulations of these two test cases. The success of this benchmarking exercise that brought together 12 teams of modellers from eight different countries all over the world constitutes in itself an indication of (i) the interest for modelling issues involving 2D sediment transport and (ii) the need for such detailed data sets. As the simulations were run without any prior knowledge of the modellers about the experimental data, the results can be considered as an overview of the capabilities of some current models, run without any calibration. This, of course, is an incomplete comparison as not all the possible modelling options were represented. However, it gives a good idea of what models are currently able to do and what should be improved or further investigated.

First, all the models were able to produce plausible results, although some could not avoid the occurrence of numerical instabilities. The water-free surface was reasonably well reproduced, with the 2D wave expansion immediately downstream of the gate and the reflections against the lateral flume walls. Most of the discrepancies may be attributed to the rough calibration of the friction coefficient, as the only available information consisted of an indicative Manning value and the mean size of the bed material.

Regarding the bed evolution, all the models predicted the scour at the dam location and deposition further downstream. However, significant discrepancies were observed in the shape of the deposition area and in the amplitude of the scour and deposition. The prediction of the bed evolution seems to be less accurate than the water level modelling.

Quite logically, it can be observed that mesh refinement allows for a significant improvement of the results, with some limitations however being observed in the mesh size: very fine meshes with sizes of 0.025 m or less are not always better than the medium-sized meshes of about 0.05 m.

Concerning the sediment transport closure equations, nothing clear is concluded at this stage. The value or formula adopted for the critical shear stress for the initiation of movement appears to be a key issue, but no "best value" was deduced from the available results. Similar conclusions arise for the transport rate formula.

As regards the governing equations themselves, no clear difference can be found between the classical or GSW approaches and the two-layer or two-phase models. A conclusion is that the present measurements do not allow for identifying any significant inertia effects that induce more differences between the models. This is mainly due to the fact that although rapid morphological changes occur with intense sediment transport, only bed load occurring in a thin sheet-flow layer is observed.

Finally, it is concluded that this modelling exercise highlights the need for further research in the field of fast transient flows involving intense sediment transport and morphological changes, as no complete agreement exists on the governing mechanisms. The fact that similar conclusions are drawn for different types of models indicates that the key problems to be investigated in transient geomorphic flow modelling lie in the closure models rather than in the governing flow equations. In particular, the link between solid transport and the depth-averaged velocity, in magnitude and in direction, is probably a key issue of 2D morphological modelling. The closure relations describing this link between hydrodynamic flow and sediment response are not universally established and often too demanding in the calibration of multiple parameters. Also, the adequacy of the Manning approach for friction losses in such fast transient cases would certainly be a question to be addressed in the future. There is still a long way for modelling in a simplified but accurate way a complex morphological evolution.

Acknowledgements

The authors thank the technicians from LEMSC and the UCL MSc students who helped in performing the experiments and measurements leading to the benchmark tests for their support, namely Pierre Henriet, David Hick, Alexandre Rouvez and

Thibaut Mahieu. The authors also thank the NSF (USA), through the PIRE project (grant no OISE 0730246), FRS-FNRS (Belgium) and the IAHR Fluvial Hydraulics Committee for providing support for the creation of the "Working group for dam-break flows over mobile beds".

Notation

C = depth-averaged concentration (–)
D = net deposition rate (m/s)
d = grain diameter (m)
E = net erosion rate (m/s)
ε_0 = porosity
g = gravity acceleration (ms^{-2})
h = flow depth (m)
n = Manning friction coefficient ($sm^{-1/3}$)
q = unit total discharge (m^2s^{-1})
q_w = unit water discharge (m^2s^{-1})
q_s = unit sediment discharge (m^2s^{-1})
ρ = density (kg/m^3)
S_f = friction slope (–)
S_o = bed slope (–)
t = time (s)
τ_c = critical shear stress ($kg\,m^{-1}\,s^{-2}$)
u = depth-averaged velocity in the x-direction (ms^{-1})
v = depth-averaged velocity in the y-direction (ms^{-1})
z_b = bed level (m)
z_w = water level (m)

Subscripts

x, y = index concerning the x- or y-direction

List of authors, in alphabetic order

Ricardo Canelas, Instituto Superior Técnico, Portugal
Zhixian Cao, Wuhan University, People's Republic of China
Luis Cea, Universidad da Coruña, Spain
Hanif M. Chaudhry, University of South Carolina, USA
Andres Die Moran, EDF, France
Kamal El Kadi, EDF, France
Rui Ferreira, Instituto Superior Técnico, Portugal
Ignacio Fraga Cadórniga, Universidad da Coruña, Spain
Noemi Gonzalez-Ramirez, RiverFlo-2D, USA
Massimo Greco, University of Naples Federico II, Italy
Wei Huang, Wuhan University, People's Republic of China
Jasim Imran, University of South Carolina, USA
Jérôme Le Coz, Cemagref, France
Reza Marsooli, University of Mississippi, USA
André Paquier, Cemagref, France
Gareth Pender, Heriot-Watt University, UK
Marianeve Pontillo, University of Naples Federico II, Italy
Jeronimo Puertas, Universidad da Coruña, Spain
Sandra Soares-Frazão, Université catholique de Louvain, Belgium
Benoit Spinewine, Université catholique de Louvain, Belgium
Catherine Swartenbroekx, Université catholique de Louvain, Belgium
Ryota Tsubaki, Hiroshima University, Japan
Catherine Villaret, EDF, France
Weiming Wu, University of Mississippi, USA
Zhiyuan Yue, Yangtze River Waterway Research Institute, People's Republic of China
Yves Zech, Université catholique de Louvain, Belgium

References

Bessenasse M., Kettab A., Paquier A. (2004). Modélisation bidimensionnelle du dépôt de sédiments dans un barrage en Algérie (Two-dimensional modeling of sediment deposits in dam reservoirs in Algeria). *La Houille Blanche* 59(1), 31–36 [in French].

Brooks, G.R., Lawrence, D.E. (1999). The drainage of the Lake Ha! Ha! Reservoir and downstream geomorphic impacts along Ha! Ha! River, Saguenay Area, Quebec, Canada. *Geomorphology* 28(1–2), 141–168.

Canelas, R. (2010). 2D mathematical modeling of discontinuous shallow sediment-laden flows. *Master Thesis*. Instituto Superior Técnico, Universidade Técnica de Lisboa, Lisboa.

Canelas, R., Ferreira, R. (2010). Workshop on dam-break flows: Description of computational model SF2D. NSF-PIRE 2010 Workshop Dam-break flow on mobile bed, private communication at http://www.uclouvain.be/373040.html, 7 p.

Cao, Z., Huang, W., Yue, Z., Pender, G. (2010). Coupled 2D mathematical modeling of dam break flow over erodible bed: UCL test case. NSF-PIRE 2010 Workshop Dam-break flow on mobile bed, private communication at http://www.uclouvain.be/373040.html, 10 p.

Cao, Z.X., Pender, G., Wallis, S., Carling, P. (2004). Computational dam-break hydraulics over erodible sediment bed, *J. Hydraulic Res.* 130(7), 689–703.

Capart, H. (2000). Dam-break induced geomorphic flows and the transition from solid- to fluid-like behaviour across evolving interfaces. *PhD thesis*. UCL, Belgium.

Capart, H., Spinewine, B., Young, D.L., Zech, Y., Brooks, G.R., Leclerc, M., Secretan, Y. (2007). The 1996 Lake Ha! Ha! breakout flood, Québec: Test data for geomorphic flood routing methods. *J. Hydraulic Res.* 45(Extra Issue), 97–109.

Cea, L., Puertas, J., Fraga, I., Trell, R., Balairon, L. (2009). Numerical modelling of the effects of river discharge regulation on the morphology and sediment transport dynamics in a shallow estuary. 33rd *IAHR Congress*, Vancouver, 3704–3711 (CD-ROM).

Cea, L., Vázquez-Cendón, M.E. (2010). Unstructured finite volume discretization of two-dimensional depth-averaged shallow water equations with porosity. *Int. J. Num. Meth. Fluids* 63(8), 903–930.

Cea, L., Fraga, I., Puertas, J. (2010). Workshop on dam-break flows: Proposed benchmark Two-dimensional dam-break flow on movable bed. NSF-PIRE 2010 workshop

'Dam-break flow on mobile bed', private communication at http://www.uclouvain.be/373040.html, 9 p.

Die Moran, A., El Kadi Abderrezzak, K., Villaret, C. (2010). Workshop Two-dimensional depth-averaged dam-break flow on mobile bed. Results submission. NSF-PIRE 2010 Workshop Dam-break flow on mobile bed, private communication at http://www.uclouvain.be/373040.html, 1 p.

Ferreira, R.M.L., Franca, M.J., Leal, J.G.A.B., Cardoso A.H. (2009). Mathematical modelling of shallow flows: Closure models drawn from grain-scale mechanics of sediment transport and flow hydrodynamics. *Canadian Journal of Civil Engineering* (CJCE), 36(10), 1605–1621.

Gonzalez-Ramirez, N. (2010). Description of benchmark simulation Two-dimensional dam-break flow on movable bed. NSF-PIRE 2010 Workshop 'Dam-break flow on mobile bed', private communication at http://www.uclouvain.be/373040.html, 13 pages.

Hervouet, J.M., Petitjean, A. (1999). Malpasset dam-break revisited with two-dimensional computations. *J. Hydraulic Res.* 37(6), 777–788.

Nguyen, D.K., Shi, Y.-E., Wang, S.S.Y., Nguyen, T.H. (2006). 2D Shallow-water model using unstructured Finite-Volumes Methods. *J. Hydraulic Eng.* 132(3), 258–269.

Paquier, A. (2009). *Logiciel Rubar* 20. Notice d'emploi. Cemagref, Unité de Recherche Hydrologie - Hydraulique, Lyon, France, 60 p. [in French].

Paquier, A., Le Coz, J. (2010). Workshop on dam-break flows. Benchmark: 2D dam-break flow on movable bed. Description of calculations performed by Cemagref. NSF-PIRE 2010 Workshop 'Dam-break flow on mobile bed', private communication at http://www.uclouvain.be/373040.html, 3 p.

Parker, G., Solari, I., Seminara, G. (2003). Bed load at low Shield stress and arbitrarily sloping beds: Alternative entrainment formulation. *Water Resources Research* 39(7), 1183–1192.

Pontillo, M., Greco, M. (2010). PIRE Benchmark. NSF-PIRE 2010 Workshop 'Dam-break flow on mobile bed', private communication at http://www.uclouvain.be/373040.html, 9 p.

Roger, S., Dewals, J., Erpicum, S., Schwanenberg, D., Schüttrumpf, H., Köngeter, J., Pirotton, M. (2009). Experimental and numerical investigations of dike-break induced flows. *J. Hydraulic Res.* 47(3), 349–459.

Shige-eda, M., Akiyama, J., Yamasaki, T. (2003). Numerical model based on FDS technique for 1D bed variation. *Annual J. Hydraulic Eng.* JSCE 47, 667–672 [in Japanese].

Soares Frazão, S., Zech, Y. (2007). Experimental study of dam-break flow against an isolated obstacle. *J. Hydraulic Res.* 45(Extra Issue), 27–36.

Soares-Frazão, S. (2010). Two-dimensional finite-volume model for shallow-water flow over fixed and mobile bed. Application to UCL benchmark 'Dam-break flow over mobile bed'. NSF-PIRE 2010 Workshop 'Dam-break flow on mobile bed', private communication at http://www.uclouvain.be/373040.html, 4 p.

Soares-Frazão, S., Zech, Y. (2011). HLLC scheme with novel wave-speed estimators appropriate for two-dimensional shallow-water flow on erodible bed. *Int. J. Num. Meth. Fluids* 66(8), 1019–1036.

Spinewine, B. (2005a). Two-layer flow behaviour and the effects of granular dilatancy in dam-break induced sheet-flow. *PhD Thesis* n°76|2005. Université catholique de Louvain, Belgium.

Spinewine, B. (2005b). Two-layer shallow water modelling of fast geomorphic flows and experimental validation on idealized laboratory dam-break waves. 31st *IAHR Congress* Seoul, 6477–6488.

Spinewine, B. (2010). UCL-Spinewine: Two-layer geomorphic shallow-water equations. NSF-PIRE 2010 Workshop 'Dam-break flow on mobile bed', private communication at http://www.uclouvain.be/373040.html, 2 p.

Swartenbroekx, C. (2010). Workshop on 2D dam-break flows over erodible bed. Brief description of a 2D two-layer model for dam-break flows. NSF-PIRE 2010 Workshop 'Dam-break flow on mobile bed', private communication at http://www.uclouvain.be/373040.html, 3 p.

Swartenbroekx, C., Soares-Frazão, S., Spinewine, B., Guinot, V., Zech, Y. (2010). Hyperbolicity preserving HLL solver for two layer shallow-water equations applied to dam-break flows. Proc. *River Flow* 2010 Braunschweig 2, 1379–1387, A. Dittrich, K. Koll, J. Aberle, P. Geisenhainer, eds.

Tsubaki, R. (2010). Description of the simulation. Workshop 'Dam-break flow on mobile bed', private communication at http://www.uclouvain.be/373040.html, 10 p.

Tsubaki, R., Fujita, I. (2010). Unstructured grid generation using LiDAR data for urban flood inundation modeling. *Hydrological Processes* 24, 1404–1420.

Valiani, A., Caleffi, V., Zanni, A. (2002). Case study Malpasset dam-break simulation using a two-dimensional Finite Volume Method. *J. Hydraulic Eng.* 128(5), 460–472.

Villaret, C., Hervouet, J.M., Huybrechts, N., Van, L.A., Davies, A.G. (2009). Effect of bed friction on morphodynamic modelling: Application to the central part of the Gironde estuary. 6th Symp. *River, Coastal and Estuarine Morphodynamics* (RCEM 2009), Santa-Fe (Argentina), 889–905.

Vischer, D.L., Hager, W.H. (1998). *Dam hydraulics*. Wiley, Chichester UK.

Wu, W., He, Z., Wang, S.S.Y. (2009). A depth-averaged 2D model of non-cohesive dam/levee breach processes. Proc. 2009 *World Environmental and Water Resources Congress* Kansas City, MO (CD-ROM).

Wu, W., Marsooli, R. (2010). Benchmark (Blind) Test of Wu's depth-averaged 2D model for dam-break flow over movable bed. NSF-PIRE 2010 Workshop 'Dam-break flow on mobile bed', private communication at http://www.uclouvain.be/373040.html, 19 p.